Bianchi, D. *et al*. (2024). *Géotechnique* **74**, No. 8, 820–828 [https://doi.org/10.1680/jgeot.22.00042]

Analysis of unsaturated seepage in infinite slopes by means of horizontal ground infiltration models

DIANA BIANCHI*, DOMENICO GALLIPOLI†, ROSSELLA BOVOLENTA‡ and MARTINO LEONI§

This paper describes a simple methodology to calculate the two-dimensional seepage across an infinite unsaturated slope using models of one-dimensional infiltration through horizontal ground. The methodology decomposes the seepage across the infinite slope into antisymmetric and symmetric parts, whose respective solutions are combined to calculate the actual flow regime. The antisymmetric solution is trivial and does not even require integration of the governing continuity equation, while the symmetric solution, albeit non-trivial, reduces to the case of one-dimensional flow through horizontal ground, for which solutions already exist. The methodology is generally applicable to the calculation of distinct seepage regimes across unsaturated slopes with different hydraulic properties under both stationary and transient conditions. The paper also defines the gradient of the piezometric head parallel to the slope, which is the Neumann boundary condition to be imposed on slope sections perpendicular to the ground surface. The rigorous definition of this gradient overcomes the need of imposing arbitrary boundary conditions in finite-element models. Finally, the paper demonstrates that all infiltrated water crosses the slope along the shortest path – namely, the path normal to the surface – while the flow parallel to the slope is entirely fed by an upstream source at infinite distance.

KEYWORDS: capillary properties; environmental engineering; geotechnical engineering; groundwater; landslides; numerical methods; partial saturation; slopes; suction

INTRODUCTION

Shallow landslides pose a serious hazard to human lives and infrastructures, not only in subtropical regions (Lim *et al*., 1996; Urciuoli *et al*., 2016; Augusto Filho & Fernandes, 2019) but almost everywhere in the world, as demonstrated by several studies published in Italy (Sanzeni *et al*., 2019; Amabile *et al*., 2020; Comegna *et al*., 2021), the UK (Balzano *et al*., 2016), Norway (L'Heureux *et al*., 2006; Melchiorre & Frattini, 2012) and the USA (Godt *et al*., 2009).

Shallow slope failures occur in the first 1–5 m of the ground, where the soil is often unsaturated and capillary (tensile) pore water pressures exist. If an unsaturated soil is wetted by meteoric precipitations, capillarity reduces and may disappear altogether as the pore water stress changes from tensile to compressive upon saturation. On the contrary, an initially saturated soil may develop capillary pressures as the degree of saturation reduces during a hot climatic spell.

Capillarity has an important effect on the mechanical behaviour of soils as it generates a cohesive component of strength, whose magnitude is directly related to the scale of the pore water tension (Fredlund & Rahardjo, 1993). This explains why changes of seepage during weather cycles have a direct impact on the activity of unstable slopes. The evaluation of the groundwater regime, and the associated evolution of pore water pressures, is therefore key to assessing the safety of slopes against sliding by means of, for example, limit equilibrium or finite-element methods (Ye *et al*., 2005; Li *et al*., 2016; Le *et al*., 2019).

The simplest landslide model assumes an infinite slope characterised by constant steepness, unlimited length and, hence, identical profiles of the soil variables along every vertical section (Skempton & DeLory, 1957). Despite its simplicity, the infinite slope model is well suited to describe shallow soil slides which take place over relatively large areas along planes that are approximately parallel to the ground surface (Zieher *et al*., 2017). The assessment of the stability of an infinite slope demands the calculation of a factor of safety, which is defined as the ratio between the available shear strength and the actual shear stress at the depth closest to failure according to the chosen constitutive law. Therefore, the evaluation of the factor of safety entails the prior calculation of the strength and stress fields inside the infinite slope, which in turn requires knowledge of the pore water field under both saturated and unsaturated conditions (Sitarenios & Casini, 2021).

The pore water field inside an infinite slope is calculated by solving the differential water continuity equation by way of either closed-form derivations (Fourie *et al*., 1999) or, if this is not possible, by way of approximated finite-element or finite-difference models (Le *et al*., 2016). This calculation is more complex under unsaturated conditions than under saturated ones because of the dependency of soil permeability and degree of saturation on pore water pressure, which introduces a degree of non-linearity in the governing equations. Despite these difficulties, rigorous analytical solutions of the one-dimensional (1D) vertical flow across horizontal unsaturated ground have been obtained by assuming different permeability and retention laws (e.g. Iverson, 2000; Lu & Griffiths, 2004; Huang & Wu, 2012). Unfortunately, the same is not true for the two-dimensional

Manuscript received 2 February 2022; revised manuscript accepted 25 May 2022. First published online ahead of print 11 July 2022. Discussion on this paper closes on 1 November 2024, for further details see p. ii.

*Dipartimento di Ingegneria Civile, Chimica e Ambientale, Università di Genova, Italy (Orcid:0000-0002-6503-0249).
†Dipartimento di Ingegneria Civile, Chimica e Ambientale, Università di Genova, Italy (Orcid:0000-0003-1576-0742).
‡Dipartimento di Ingegneria Civile, Chimica e Ambientale, Università di Genova, Italy (Orcid:0000-0001-8099-0865).
§Dipartimento di Ingegneria Civile, Chimica e Ambientale, Università di Genova, Italy (Orcid:0000-0002-7984-1085).

(2D) flow across an infinite unsaturated slope, whose seepage regime has been analytically solved only by a handful of studies that assume exponential permeability and retention laws (Lu & Godt, 2008; Travis *et al.*, 2010; Zhan *et al.*, 2013). Most often, the unsaturated flow across an infinite slope has been evaluated by way of numerical (i.e. finite-element or finite-difference) models that represent a segment of the inclined soil layer (e.g. Griffiths *et al.*, 2011). To be viable, these models impose arbitrary boundary conditions (typically hydrostatic or impermeable) on the two end sides that cut across the slope (Cho & Lee, 2002; El Shamy, 2007). The inaccuracies introduced by this artefact are usually minimised by: (*a*) calculating the flow regime at the middle section of the model, which is the farthest section from the boundaries where the arbitrary conditions have been imposed and (*b*) by modelling a relatively slender slope segment with length-to-thickness ratio larger than 20 (Milledge *et al.*, 2012).

This paper presents a methodology that improves and simplifies the calculation of the 2D seepage across an unsaturated infinite slope compared to current numerical models, thus overcoming the above limitations. This is achieved by decomposing the flow regime into antisymmetric and symmetric parts, which correspond to the two components of the specific water weight that are parallel and perpendicular to the slope, respectively (Fig. 1). The antisymmetric part is immediately solved, without even integrating the governing partial differential equations, because the pore water pressure field is zero everywhere due to the antisymmetric nature of the problem. Conversely, the symmetric part reduces to the case of 1D vertical infiltration across horizontal ground, for which analytical and numerical solutions are already available.

The proposed methodology has practical relevance and presents the following elements of novelty as discussed later.

(*a*) It extends existing solutions of 1D vertical flow across horizontal ground to the study of 2D seepage across an infinite slope. Recall that, owing to symmetry, an impermeable condition applies to the vertical boundaries of 1D flow models.
(*b*) It defines the piezometric head gradient along the slope direction, that is the Neumann boundary condition to be imposed on slope sections perpendicular to the ground. This boundary condition allows a rigorous flow analysis by modelling only a narrow slope slice.
(*c*) It provides a physical interpretation of the seepage regime across an infinite slope showing that the flow parallel to the ground is entirely fed by an upstream source at infinite distance, whereas the flow perpendicular to the ground is entirely fed by surface infiltration.

For the sake of brevity, the proposed methodology has only been validated for the case of steady-state flow across an unsaturated slope with an exponential permeability law. Nevertheless, the approach is entirely general and can be equally adopted for studying the transient flow regime across unsaturated slopes with different hydraulic laws, including hysteretic ones.

DECOMPOSITION OF FLOW REGIME INTO ANTISYMMETRIC AND SYMMETRIC PARTS

Figure 1 shows a schematic representation of an infinite unsaturated slope of constant thickness L (measured perpendicular to the surface) permeated by water and forming an angle β with respect to the horizontal. The slope is made of a homogeneous unsaturated soil with permeability $K(u)$

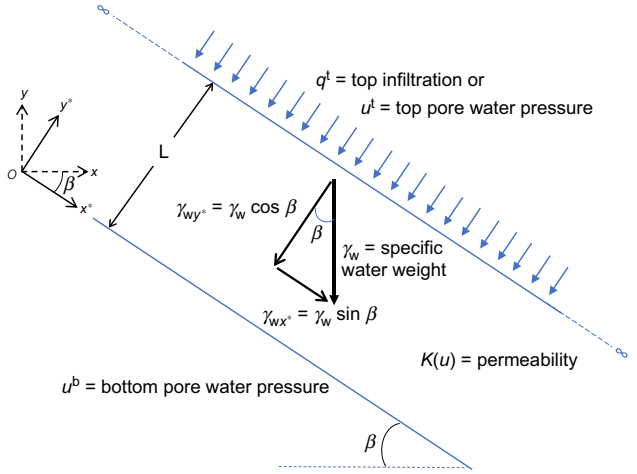

Fig. 1. Geometry of infinite unsaturated slope permeated by water with hydraulic boundary conditions

that depends on the pore water pressure u according to the following law

$$K(u) = \kappa_r(u) K_{sat} \tag{1}$$

where $\kappa_r(u)$ is the relative permeability and K_{sat} is the saturated permeability. The relative permeability $\kappa_r(u)$ is a function of the pore water pressure u and defines the dependency of soil permeability on the saturation state. The relative permeability is equal to one when the soil is saturated and the pore water pressure is non-negative, whereas it tends towards zero as the soil desaturates and the pore water pressure decreases over the negative range. Recall that, in unsaturated soils, the pore water is under tension and the corresponding pressure u is negative according to geotechnical convention.

The relative permeability is usually expressed as a function of soil suction $s = u_a - u$, which is the difference between pore air pressure u_a and pore water pressure u. In this study, however, it is assumed that the pore air pressure is atmospheric – that is, $u_a = 0$ – so that the suction reduces to the pore water pressure change of sign – that is, $s = -u$ – which is the reason why the relative permeability is expressed as a function of pore water pressure u rather than suction s.

The saturated permeability K_{sat} in equation (1) is constant and defined as

$$K_{sat} = \frac{\kappa\, \gamma_w}{\mu} \tag{2}$$

where κ is the intrinsic permeability of the soil; γ_w is the specific weight of the water; and μ is the dynamic viscosity of the water.

The infinite slope of Fig. 1 is subjected to a constant pore water pressure u^b at the bottom, and to either a constant pore water pressure u^t or a constant infiltration rate q^t (perpendicular to the ground) at the top. The chosen reference system (O, x^*, y^*) has its origin O on the bottom boundary of the slope and is defined by the axes x^* and y^*, which are respectively parallel and perpendicular to the ground surface. This reference system is therefore rotated by an angle β with respect to the reference system (O, x, y), which has the same origin O but is defined by the axes x and y aligned with the horizontal and vertical directions, respectively.

The specific water weight γ_w has vertical direction and can, therefore, be broken up into the two components $\gamma_{wx^*} = \gamma_w \sin\beta$ and $\gamma_{wy^*} = \gamma_w \cos\beta$ that are respectively parallel and perpendicular to the slope – that is the components along the x^* and y^* axes. This enables the decomposition of the flow

regime into two parts, namely, an antisymmetric part and a symmetric part, which can be separately analysed. The results from the analysis of each one of these two parts can then be combined to provide the solution of the actual flow problem.

Antisymmetric part

Figure 2 shows the antisymmetric part of the flow regime, where $\gamma_{wx^*} = \gamma_w \sin\beta$ is the antisymmetric component of the specific water weight acting in the direction parallel to the slope. The antisymmetric fields of pore water pressure u^{asym}, piezometric head h^{asym}, flux component parallel to the slope $q_{x^*}^{asym}$ and flux component perpendicular to the slope $q_{y^*}^{asym}$ are calculated next.

Because the ground extends indefinitely in the direction parallel to the slope, every line that is normal to the surface is an axis of antisymmetry. This means that the antisymmetric pore water pressure field must be zero everywhere – that is $u^{asym} = 0$ – because, if it was different from zero, the antisymmetry of the problem would be violated. It is therefore unnecessary to solve the governing continuity equation to calculate the antisymmetric pore water pressure field because this is a priori equal to zero.

Given that $u^{asym} = 0$, the antisymmetric piezometric head h^{asym} is

$$h^{asym} = -x^* + \frac{u^{asym}}{\gamma_{wx^*}} = -x^* \tag{3}$$

where a minus sign is introduced before the coordinate x^* because the antisymmetric specific water weight γ_{wx^*} has the same direction of the x^* axis. This is different from the symmetric case where the component of the specific water weight normal to the slope γ_{wy^*} has opposite direction with respect to the y^* axis (see Fig. 1). The piezometric head coincides with the total head if the kinetic energy is assumed negligible, which is customary in ground flow analyses.

Owing to the antisymmetric nature of the problem, the component of the flux vector normal to the slope is zero, – that is, $q_{y^*}^{asym} = 0$ – and only the component parallel to the slope is different from zero – that is, $q_{x^*}^{asym} \neq 0$. The flux component parallel to the slope $q_{x^*}^{asym}$ can be calculated by applying Darcy's law to the antisymmetric piezometric head h^{asym} of equation (3) as

$$q_{x^*}^{asym} = -K^{asym}(u)\frac{\partial h^{asym}}{\partial x^*} = K^{asym}(u) \tag{4}$$

The antisymmetric unsaturated permeability $K^{asym}(u)$ of equation (4) is calculated from the unsaturated permeability expression of equation (1) where the saturated permeability K_{sat} is replaced with the corresponding antisymmetric value K_{sat}^{asym} as

$$K^{asym}(u) = \kappa_r(u) K_{sat}^{asym} \tag{5}$$

In turn, the antisymmetric saturated permeability K_{sat}^{asym} of equation (5) is calculated from the saturated permeability expression of equation (2) where the specific water weight γ_w is replaced with the antisymmetric value $\gamma_{wx^*} = \gamma_w \sin\beta$ as

$$K_{sat}^{asym} = \frac{\kappa\,\gamma_{wx^*}}{\mu} = \frac{\kappa\,\gamma_w}{\mu}\sin\beta = K_{sat}\sin\beta \tag{6}$$

By substituting equation (6) into equation (5) and taking into account equation (1), the antisymmetric unsaturated permeability $K^{asym}(u)$ is expressed in terms of the unsaturated permeability $K(u)$ as

$$K^{asym}(u) = \kappa_r(u)\, K_{sat}\sin\beta = K(u)\sin\beta \tag{7}$$

Finally, by substituting equation (7) into equation (4), the antisymmetric flux parallel to the slope $q_{x^*}^{asym}$ is calculated in terms of the unsaturated permeability $K(u)$ as

$$q_{x^*}^{asym} = K(u)\sin\beta \tag{8}$$

Note that the antisymmetric unsaturated permeability $K^{asym}(u)$ inside equation (4) is a material property and therefore depends on the actual pore water pressure field u, which will be shown later to coincide with the symmetric pore water pressure field.

Symmetric part

Figure 3 shows the symmetric part of the flow regime where $\gamma_{wy^*} = \gamma_w \cos\beta$ is the symmetric component of the specific water weight in the direction normal to the slope, while the top and bottom boundary conditions are those of the actual problem. The symmetric fields of pore water pressure u^{sym}, piezometric head h^{sym}, flux component parallel to the slope $q_{x^*}^{sym}$ and flux component perpendicular to the slope $q_{y^*}^{sym}$ are calculated next.

As the soil geometry extends indefinitely in the direction parallel to the slope, every line that is normal to the ground constitutes an axis of symmetry. This means that the symmetric pore water pressure field u^{sym} depends only on the y^* coordinate, which is perpendicular to the slope while it is constant along the x^* coordinate, which is parallel to the slope.

Considering that $\gamma_{wy^*} = \gamma_w \cos\beta$, the symmetric piezometric head h^{sym} is calculated as

$$h^{sym} = y^* + \frac{u^{sym}}{\gamma_{wy^*}} = y^* + \frac{u^{sym}}{\gamma_w \cos\beta} \tag{9}$$

Owing to symmetry, the component of the flux vector parallel to the slope is zero – that is, $q_{x^*}^{sym} = 0$ – and only the

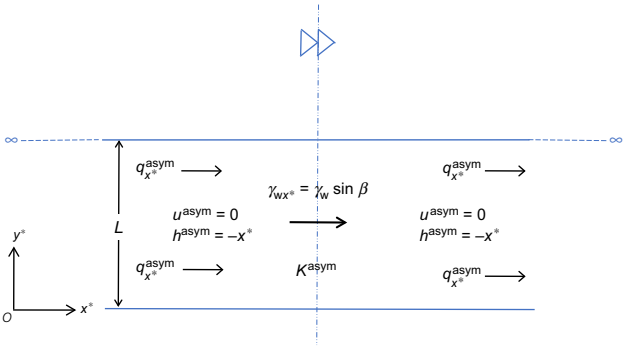

Fig. 2. Antisymmetric part of the flow regime across an infinite slope

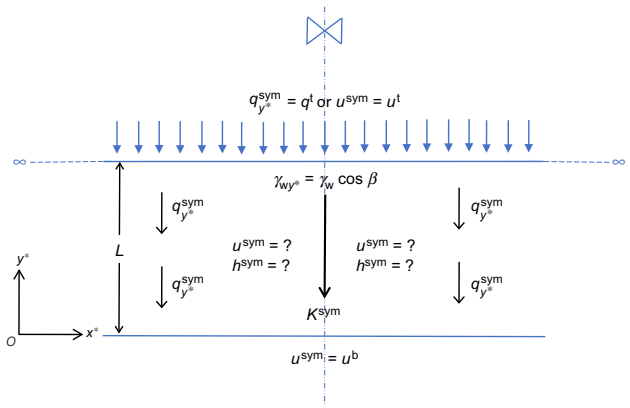

Fig. 3. Symmetric part of the flow regime across an infinite slope

component normal to the slope is different from zero – that is, $q_{y^*}^{\text{sym}} \neq 0$. The flux component $q_{y^*}^{\text{sym}}$ can be calculated by way of Darcy's law from the symmetric piezometric head h^{sym} of equation (9) as

$$q_{y^*}^{\text{sym}} = -K^{\text{sym}}(u)\frac{\partial h^{\text{sym}}}{\partial y^*} = -K^{\text{sym}}(u)\left(1+\frac{1}{\gamma_{\text{w}}\cos\beta}\frac{\partial u^{\text{sym}}}{\partial y^*}\right) \tag{10}$$

As before, the symmetric unsaturated permeability $K^{\text{sym}}(u)$ inside equation (10) is calculated from the unsaturated permeability expression of equation (1) where the saturated permeability K_{sat} is replaced with the corresponding symmetric value $K_{\text{sat}}^{\text{sym}}$ as

$$K^{\text{sym}}(u) = \kappa_{\text{r}}(u)\ K_{\text{sat}}^{\text{sym}} \tag{11}$$

Similarly, the symmetric saturated permeability $K_{\text{sat}}^{\text{sym}}$ inside equation (11) is obtained from the saturated permeability expression of equation (2) after replacing the specific water weight γ_{w} with the symmetric value $\gamma_{\text{w}y^*} = \gamma_{\text{w}}\cos\beta$ as

$$K_{\text{sat}}^{\text{sym}} = \frac{\kappa\,\gamma_{\text{w}y^*}}{\mu} = \frac{\kappa\,\gamma_{\text{w}}}{\mu}\cos\beta = K_{\text{sat}}\cos\beta \tag{12}$$

By substituting equation (12) into equation (11) and taking into account equation (1), the symmetric unsaturated permeability $K^{\text{sym}}(u)$ is expressed in terms of the unsaturated permeability $K(u)$ as

$$K^{\text{sym}}(u) = \kappa_{\text{r}}(u)K_{\text{sat}}\cos\beta = K(u)\ \cos\beta \tag{13}$$

which is substituted inside equation (10) to yield the following expression of the symmetric flux perpendicular to the slope $q_{y^*}^{\text{sym}}$ in terms of the unsaturated permeability $K(u)$

$$q_{y^*}^{\text{sym}} = -K(u)\ \cos\beta\left(1+\frac{1}{\gamma_{\text{w}}\cos\beta}\frac{\partial u^{\text{sym}}}{\partial y^*}\right) \tag{14}$$

The symmetric unsaturated permeability $K^{\text{sym}}(u)$ inside equation (10) is a material property and therefore depends on the actual pore water pressure field u by way of the relative permeability function of equation (1). It will be shown later that the actual and symmetric pore water pressure fields coincide, which means that the flux $q_{y^*}^{\text{sym}}$ of equation (14) can equally be written in terms of the symmetric pore water pressure field u^{sym} as

$$q_{y^*}^{\text{sym}} = -K(u^{\text{sym}})\ \cos\beta\left(1+\frac{1}{\gamma_{\text{w}}\cos\beta}\frac{\partial u^{\text{sym}}}{\partial y^*}\right) \tag{15}$$

This is important because it means that the symmetric seepage of Fig. 3 reduces to the case of 1D flow across horizontal ground and can therefore be solved by way of vertical infiltration models, provided that the symmetric values of water specific weight $\gamma_{\text{w}}\cos\beta$ and permeability $K(u^{\text{sym}})\cos\beta$ are considered.

Finally, the decomposition of the flow regime into antisymmetric and symmetric parts allows a physical interpretation of the water movement in the directions parallel and perpendicular to the slope, respectively. Inspection of Fig. 2 indicates that the flow in the direction parallel to the slope is entirely fed by an upstream source located at infinite distance with no contribution from surface infiltration. Conversely, inspection of Fig. 3 indicates that the flow in the direction perpendicular to the slope is entirely fed by surface infiltration, with no contribution from the upstream region. In other words, all water that infiltrates the surface crosses the slope thickness along the shortest path, which is the path perpendicular to the ground.

Combination of symmetric and antisymmetric parts

The previous antisymmetric and symmetric flow fields are now combined to obtain the actual flow field across the infinite slope. To this end, it is observed that the component of the actual flux parallel to the slope, q_{x^*}, coincides with the same component of the antisymmetric flux, $q_{x^*}^{\text{asym}}$, given by equation (8) because the symmetric component, $q_{x^*}^{\text{sym}}$, is zero

$$q_{x^*} = q_{x^*}^{\text{asym}} = K(u)\sin\beta \tag{16}$$

Conversely, the component of the actual flux perpendicular to the slope, q_{y^*}, coincides with the same component of the symmetric flux, $q_{y^*}^{\text{sym}}$, given by equation (14) because the antisymmetric component, $q_{y^*}^{\text{asym}}$, is zero

$$q_{y^*} = q_{y^*}^{\text{sym}} = -K(u)\cos\beta\left(1+\frac{1}{\gamma_{\text{w}}\cos\beta}\frac{\partial u^{\text{sym}}}{\partial y^*}\right) \tag{17}$$

Now consider that the two components of the actual flux parallel and perpendicular to the slope can be alternatively calculated by way of Darcy's law from the actual piezometric head h as

$$q_{x^*} = -K(u)\frac{\partial h}{\partial x^*} \tag{18}$$

$$q_{y^*} = -K(u)\frac{\partial h}{\partial y^*} \tag{19}$$

By equating the right-hand sides of equations (16) and (17) with the right-hand sides of equations (18) and (19), respectively, the components of the gradient of the piezometric head h along the directions parallel and normal to the slope are obtained as

$$\frac{\partial h}{\partial x^*} = -\sin\beta \tag{20}$$

$$\frac{\partial h}{\partial y^*} = \cos\beta + \frac{1}{\gamma_{\text{w}}}\frac{\partial u^{\text{sym}}}{\partial y^*} \tag{21}$$

Note that equation (20) provides the constant Neumann boundary condition for all sections perpendicular to the slope. This boundary condition can also be expressed in terms of pore water pressure as

$$\frac{\partial u}{\partial x^*} = 0 \tag{22}$$

Finally, because the symmetric pore water pressure u^{sym} depends only on the y^* coordinate, the piezometric head h can be calculated by summing the integrals of the two gradient components of equations (20) and (21) as

$$h = -\sin\beta x^* + \cos\beta y^* + \frac{u^{\text{sym}}}{\gamma_{\text{w}}} \tag{23}$$

The substitution of both the expression of the piezometric head h given by equation (23) and the coordinate transformation $y = \cos\beta y^* - \sin\beta x^*$ inside the definition of pore water pressure

$$u = \gamma_{\text{w}}(h-y) \tag{24}$$

yields the equality

$$u = \gamma_{\text{w}}\left(-\sin\beta x^* + \cos\beta y^* + \frac{u^{\text{sym}}}{\gamma_{\text{w}}} - \cos\beta y^* + \sin\beta x^*\right) = u^{\text{sym}} \tag{25}$$

which demonstrates the coincidence between the actual and symmetric pore water pressure fields – that is, $u = u^{\text{sym}}$, as anticipated above.

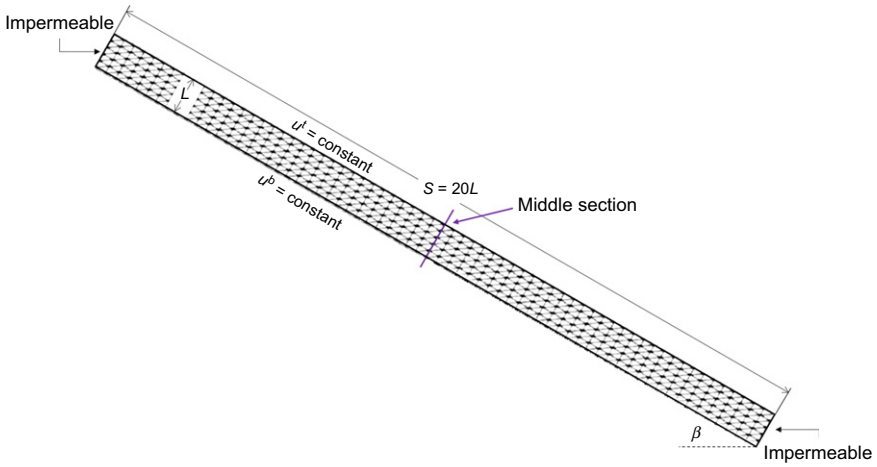

Fig. 4. Model of infinite slope in Plaxis 2D

VALIDATION OF PROPOSED METHODOLOGY

The proposed methodology is here applied to the analysis of steady-state flow inside an infinite unsaturated slope. The symmetric part of the flow regime is calculated using the closed-form solution of Lu & Griffiths (2004), who studied the steady-state vertical infiltration across a horizontal homogeneous unsaturated soil layer of thickness L. Lu & Griffiths (2004) assumed the following exponential relative permeability function that decreases with increasing suction or, if the pore air pressure is zero as in this study, with decreasing pore water pressure

$$K(u) = \kappa_r(u)K^{sat} = e^{\alpha u}K^{sat} \tag{26}$$

where α is a soil parameter whose magnitude governs the rate of permeability decrease with reducing pore water pressure u. Recall that, in unsaturated soils, the pore water pressure is tensile and therefore negative, which means that the unsaturated permeability calculated by equation (26) is smaller than the saturated value.

Lu & Griffiths (2004) assumed a zero pore water pressure at the bottom of the horizontal soil layer and a constant infiltration rate at the top. In this paper, however, their solution has been reworked in a more general form to allow the imposition of any boundary condition, at the top and bottom of the soil layer, in terms of either infiltration rate or pore water pressure. In particular, the distribution of the pore water pressure u across the horizontal soil layer has been here integrated again as

$$u = \frac{\ln\left(e^{\alpha\gamma_w y^*} + C_1\right) - \alpha\gamma_w y^*}{\alpha} + C_2 \tag{27}$$

which is more general than the expression of Lu & Griffiths (2004) as it allows the imposition of any boundary condition by calculating the corresponding expressions of the two constants of integrations C_1 and C_2. For example, if a pore water pressure u^b is imposed at the bottom boundary and an infiltration rate q^t is imposed at the top boundary, the pore water pressure u inside the horizontal soil layer is calculated from equation (27) as

$$u = \frac{1}{\alpha}\left\{\ln\left[e^{-\alpha\gamma_w y^*}\left(e^{\alpha u^b} + \frac{q^t}{K^{sat}}\right) - \frac{q^t}{K^{sat}}\right]\right\} \tag{28}$$

Instead, if two pore water pressures u^b and u^t are respectively imposed at the bottom and top boundaries, the expression of u is obtained from equation (27) as

$$u = \frac{1}{\alpha}\ln\frac{1 - e^{\alpha\gamma_w(L-y^*)}\left(1 - e^{\alpha(u^t-u^b)}\right) - e^{\alpha(\gamma_w L+u^t-u^b)}}{1 - e^{\alpha\gamma_w L}} + u^b \tag{29}$$

Thus, equations (28) and (29) provide the solution of the 1D vertical flow across a horizontal unsaturated soil layer for two distinct sets of boundary conditions.

The symmetric seepage across an infinite slope having thickness L and the permeability law of equation (26) can therefore be calculated from equations (28) and (29) after replacing the specific water weight γ_w and saturated permeability K^{sat} with the corresponding symmetric values $\gamma_{wy^*} = \gamma_w \cos\beta$ and $K^{sat}_{y^*} = K^{sat}\cos\beta$. This substitution results in the following two expressions of the symmetric pore water pressure field, which also coincides with the actual pore pressure field as discussed before

$$u^{sym} = u = \frac{1}{\alpha}\ln\left[e^{-\alpha\,\gamma_w\cos\beta\,y^*}\left(e^{\alpha u^b} + \frac{q^t}{K^{sat}\cos\beta}\right) - \frac{q^t}{K^{sat}\cos\beta}\right] \tag{30}$$

$$u^{sym} = u = \frac{1}{\alpha}\ln\frac{1 - e^{\alpha\,\gamma_w\cos\beta(L-y^*)}\left(1 - e^{\alpha(u^t-u^b)}\right) - e^{\alpha(\gamma_w\cos\beta\,L+u^t-u^b)}}{1 - e^{\alpha\,\gamma_w\cos\beta\,L}} + u^b \tag{31}$$

The pore water pressure u calculated from either equation (30) or (31) can then be substituted inside equation (23) to obtain the corresponding piezometric head h, which is then introduced inside equations (18) and (19) to obtain the fluxes parallel and perpendicular to the slope, namely, q_{x^*} and q_{y^*}.

Equation (30) is here validated against the work by Zhan *et al.* (2013), who provided the analytical solution of transient seepage across an infinite unsaturated slope with the same exponential permeability law of equation (26). The slope of Zhan *et al.* (2013) is subjected to a constant pore water pressure at the bottom and a constant infiltration rate at the top, which are the same boundary conditions as equation (30). Unlike the present work, Zhan *et al.* (2013) derived their solution in terms of pressure head u/γ_w rather than pressure u and assumed the infiltration q^t as vertical

downwards positive rather than perpendicular to the slope upwards positive. Once these differences are accounted for, equation (30) coincides with the analogous solution by Zhan *et al.* (2013) when time tends to infinity and, hence, the flow regime tends towards stationary conditions. This coincidence between the two solutions provides an initial validation of the proposed methodology of partitioning the flow regime into antisymmetric and symmetric parts.

Equation (31) calculates instead the seepage regime when two pore water pressures u^{b} and u^{t} are imposed at the bottom and top boundaries, thus it is here validated against a finite-element model of a slender slope segment, as shown in Fig. 4. The segment has inclination $\beta = 30°$, thickness $L = 5\,\text{m}$, length $S = 100\,\text{m}$ and, hence, a length-to-thickness ratio $(S/L) = 20$, which is large enough to mimic the behaviour of an infinite slope. The model incorporates the same permeability law as equation (26) and has been finely meshed with 15-noded triangular elements using the geotechnical finite-element software Plaxis 2D rel. 2019 (Fig. 4). Two arbitrary zero flow conditions are imposed on the left and right boundaries of the model while the pore water pressure is calculated at the middle section, which is assumed far enough from these two boundaries to neglect any influence. The values of all geometrical and material parameters are summarised in Table 1.

Figure 5 compares the steady-state pore water pressure profiles (normal to the ground) calculated by both equation (31) and the finite-element model of Fig. 4 for two different sets of boundary conditions corresponding to $u^{b} = 0\,\text{kPa}$ and $u^{t} = -100\,\text{kPa}$ in one case and $u^{b} = 0\,\text{kPa}$ and $u^{t} = -50\,\text{kPa}$ in the other case. The perfect match between the results of equation (31) and the finite-element model confirms the validity of the proposed methodology.

If the arbitrary zero flow condition on the left and right boundaries is replaced with the rigorous Neumann condition

Table 1. Geometric and material parameters

L: m	5·00
β: degrees	30·00
S/L	20·00
K^{sat}: m/s	3×10^{-6}
α: 1/kPa	0·10
γ_w: kN/m^3	10·00

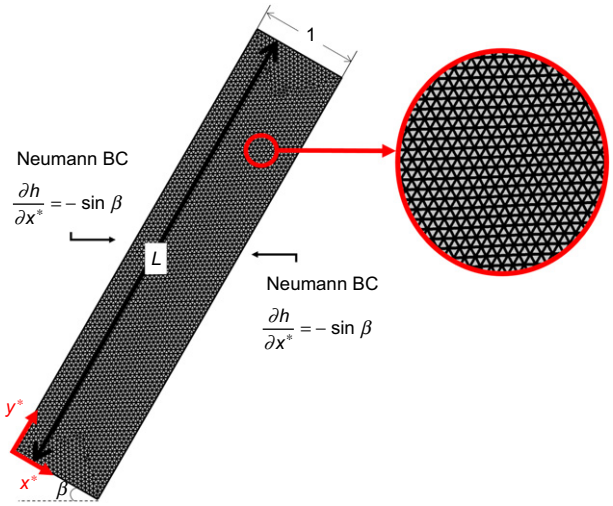

Fig. 6. Model of infinite slope in Comsol Multiphysics

of equation (20), the finite-element model can be significantly reduced in size from a large (slender) slope segment to a narrow (squat) slope slice. To demonstrate this, a finite-element model of a narrow slope slice, with unit length, has been discretised using three-noded triangular elements in the software Comsol Multiphysics 5·6 rel. 2020 (Fig. 6). This model has then been used to solve the following stationary form of Richards' equation

$$\nabla \cdot (K \nabla h) = 0 \tag{32}$$

while imposing the Neumann boundary condition of equation (20) on the two sides perpendicular to the ground. Prior to that, the permeability law of equation (26) has been recast in terms of piezometric head h (rather than pore water pressure u) for consistency with equation (32) as

$$K(h) = \kappa_r(h) K^{sat} = e^{\alpha \gamma_w (h-y)} K^{sat} \tag{33}$$

As before, all geometrical and material parameters of the model are given in Table 1.

Two sets of boundary conditions have been imposed on the top and bottom boundaries of the slope slice corresponding to $u^{b} = 0\,\text{kPa}$ and $u^{t} = -100\,\text{kPa}$ in one case and $u^{b} = 0\,\text{kPa}$

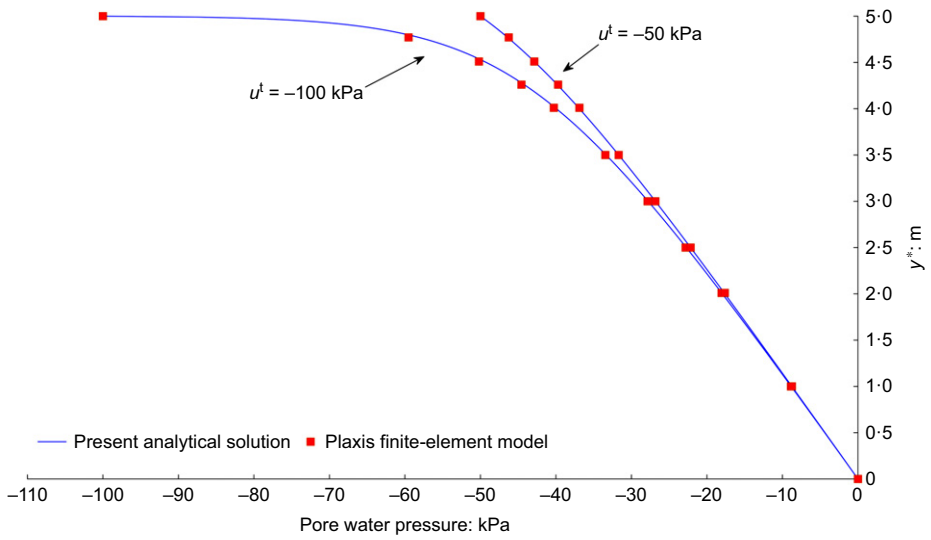

Fig. 5. Comparison between present analytical solution and Plaxis finite-element model for constant pore water pressures at the top and bottom of the infinite slope

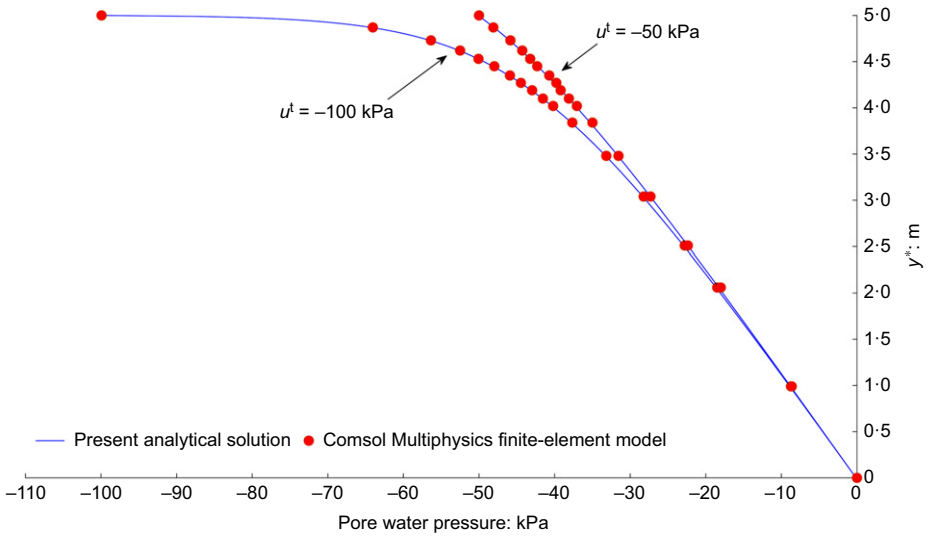

Fig. 7. Comparison between present analytical solution and Comsol Multiphysics finite-element model for constant pore water pressure at the top and bottom of the infinite slope

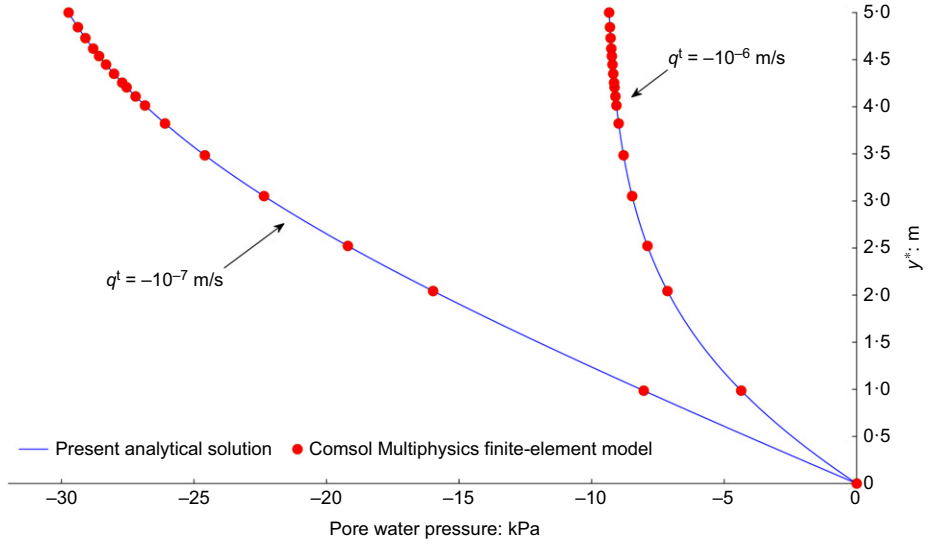

Fig. 8. Comparison between present analytical solution and Comsol Multiphysics finite-element model for constant infiltration rate at the top and constant pore water pressure at the bottom of the infinite slope

and $u^t = -50$ kPa in the other case. Fig. 7 shows the perfect match of the pressure profiles calculated by equation (31) and the Comsol Multiphysics software for both sets of boundary conditions, which confirms the correctness of the Neumann expression of equation (20).

A further validation has been performed by imposing an infiltration rate q^t on the top boundary, as in the case of equation (30). In particular, two distinct sets of boundary conditions have been imposed corresponding to $u^b = 0$ kPa and $q^t = -10^{-7}$(m/s) in one case and $u^b = 0$ kPa and $q^t = -10^{-6}$(m/s) in the other case. Fig. 8 shows that the Comsol Multiphysics results perfectly match the solution of equation (30), thus confirming the ability of the Neumann boundary condition of equation (20) to obtain the exact pore water pressure profile even when a model of reduced size is employed.

Although the proposed methodology has been validated only for stationary flow conditions with an exponential permeability law, the approach is also applicable to the study of transient flow across infinite slopes obeying different hydraulic laws, including hysteretic ones.

CONCLUSIONS

Very few closed-form solutions of 2D flow across an infinite unsaturated slope have been derived by assuming simple hydraulic laws. More frequently, the flow regime has been evaluated by way of numerical (i.e. finite-element or finite-difference) models, which discretise a relatively large segment of the infinite slope to minimise errors attributable to the imposition of arbitrary boundary conditions at the domain ends. This paper has illustrated a simple methodology that overcomes the above limitations by extending solutions of 1D vertical infiltration across horizontal unsaturated ground to the case of 2D seepage across an infinite slope.

The methodology relies on the decomposition of the seepage across the infinite slope into two parts, an antisymmetric part and a symmetric part, whose respective solutions are then combined to define the actual 2D flow regime. The solution of the antisymmetric part is trivial and does not even require integration of the governing water continuity equation. Conversely, the solution of the symmetric part is non-trivial, but it reduces to the simpler case of vertical

flow across horizontal ground, for which analytical and numerical solutions already exist with a variety of hydraulic laws.

The paper also defines the gradient of piezometric head along the slope direction, which is the Neumann boundary condition to be imposed on the slope sections that are perpendicular to the ground surface. By imposing this rigorous boundary condition, the seepage regime can be calculated by way of a finite-element or finite-difference model of a narrow slope slice. This enables considerable computational savings compared to current practice where a large slope segment is discretised to compensate for the arbitrariness of the boundary conditions at the model ends.

The present work also offers a physical interpretation of the flow regime across an infinite slope by differentiating between the sources of the seepage parallel and perpendicular to the slope. It emerges that the flow parallel to the slope is entirely fed by an upstream source located at infinite distance, whereas the flow perpendicular to the slope is entirely fed by infiltration at the ground surface. This means that all ground infiltration crosses the slope along the shortest possible path, which is the path perpendicular to the ground.

The above conclusions are applicable to all infinite slopes regardless of whether the flow regime is stationary or transient and regardless of the chosen permeability/retention law, which can also be hysteretic. Future research will concentrate on the application of the above methodology to the calculation of the factor of safety in shallow slopes by further exploiting the proposed partition into antisymmetric and symmetric components.

NOTATION

C_1, C_2 constants of integration
h piezometric head
h^{asym} antisymmetric piezometric head
h^{sym} symmetric piezometric head
K permeability
K^{asym} antisymmetric permeability
K^{sym} symmetric permeability
K_{sat} saturated permeability
K_{sat}^{asym} antisymmetric saturated permeability
K_{sat}^{sym} symmetric saturated permeability
L slope thickness
(O, x, y) standard reference system
(O, x^*, y^*) rotated reference system
q^t infiltration rate normal to the ground surface
$q_{x^*}^{asym}$ component parallel to the slope of the antisymmetric flux vector
$q_{x^*}^{sym}$ component parallel to the slope of the symmetric flux vector
$q_{y^*}^{asym}$ component normal to the slope of the antisymmetric flux vector
$q_{y^*}^{sym}$ component normal to the slope of the symmetric flux vector
S slope length
s suction
u pore water pressure
u_a pore air pressure
u^b bottom pore water pressure
u^{asym} antisymmetric pore water pressure
u^{sym} symmetric pore water pressure
u^t top pore water pressure
α unsaturated permeability parameter
β slope angle
γ_w specific weight of water
γ_{wx^*} component parallel to the slope of the specific weight of water
γ_{wy^*} component normal to the slope of the specific weight of water
κ intrinsic permeability
κ_r relative permeability
μ dynamic viscosity of water

REFERENCES

Amabile, A., Pozzato, A. & Tarantino, A. (2020). Instability of flood embankments due to pore-water pressure build-up at the toe: lesson learned from the Adige River case study. *Can. Geotech. J.* **57**, No. 12, 1844–1853, https://doi.org/10.1139/cgj-2018-0372.

Augusto Filho, O. & Fernandes, M. A. (2019). Landslide analysis of unsaturated soil slopes based on rainfall and matric suction data. *Bull. Engng Geol. Environ.* **78**, No. 6, 4167–4185, https://doi.org/10.1007/s10064-018-1392-5.

Balzano, B., Tarantino, A. & Ridley, A. (2016) Analysis of a rainfall-triggered landslide at rest and be thankful in Scotland. In *3rd European conference on unsaturated soils – "E-UNSAT 2016"* (eds P. Delage, Y.-J. Cui, S. Ghabezloo, J.-M. Pereira and A.-M. Tang), E3S Web of Conferences vol. 9, article 15009, https://doi.org/10.1051/e3sconf/20160915009. Les Ulis, France: EDP Sciences.

Cho, S. E. & Lee, S. R. (2002). Evaluation of surficial stability for homogeneous slopes considering rainfall characteristics. *J. Geotech. Geoenviron. Engng* **128**, No. 9, 756–763, https://doi.org/10.1061/(ASCE)1090-0241(2002)128:9(756).

Comegna, L., Damiano, E., Greco, R., Olivares, L. & Picarelli, L. (2021). The hysteretic response of a shallow pyroclastic deposit. *Earth Syst. Sci. Data* **13**, No. 6, 2541–2553, https://doi.org/10.5194/essd-13-2541-2021.

El Shamy, U. (2007) Numerical study of rainfall infiltration in unsaturated slopes. In *Embankments, dams, and slopes* (eds F. Silva-Tulla and P. G. Nicholson), GSP 161, pp. 1–10, https://doi.org/10.1061/40905(224)4. Reston, VA, USA: American Society of Civil Engineers.

Fourie, A. B., Rowe, D. & Blight, G. E. (1999). The effect of infiltration on the stability of the slopes of a dry ash dump. *Géotechnique* **49**, No. 1, 1–13, https://doi.org/10.1680/geot.1999.49.1.1.

Fredlund, D. G. & Rahardjo, H. (1993). *Soil mechanics for unsaturated soils*. New York, NY, USA: John Wiley & Sons.

Godt, J. W., Baum, R. L. & Lu, N. (2009). Landsliding in partially saturated materials. *Geophys. Res. Lett.* **36**, No. 2, L02403, https://doi.org/10.1029/2008GL035996.

Griffiths, D. V., Huang, J. & deWolfe, G. F. (2011). Numerical and analytical observations on long and infinite slopes. *Int. J. Numer. Analyt. Methods Geomech.* **35**, No. 5, 569–585, https://doi.org/10.1002/nag.909.

Huang, R. Q. & Wu, L. Z. (2012). Analytical solutions to 1-D horizontal and vertical water infiltration in saturated/unsaturated soils considering time-varying rainfall. *Comput. Geotech.* **39**, 66–72, https://doi.org/10.1016/j.compgeo.2011.08.008.

Iverson, R. M. (2000). Landslide triggering by rain infiltration. *Water Resour. Res.* **36**, No. 7, 1897–1910, https://doi.org/10.1029/2000WR900090.

Le, T. M. H., Gallipoli, D., Sanchez, M. & Wheeler, S. (2016) Characteristics of failure mass and safety factor during rainfall of an unsaturated slope. In *3rd European conference on unsaturated soils – "E-UNSAT 2016"* (eds P. Delage, Y.-J. Cui, S. Ghabezloo, J.-M. Pereira and A.-M. Tang), E3S Web of Conferences vol. 9, article 15011, https://doi.org/10.1051/e3sconf/20160915011. Les Ulis, France: EDP Sciences.

Le, T. M. H., Sanchez, M., Gallipoli, D. & Wheeler, S. (2019). Probabilistic study of rainfall-triggered instabilities in randomly heterogeneous unsaturated finite slopes. *Transp. Porous Media* **126**, No. 1, 199–222, https://doi.org/10.1007/s11242-018-1140-0.

L'Heureux, J. S., Høeg, K. & Høydal, Ø. A. (2006) Numerical analyses and field case study of slope subjected to rainfall. In *Unsaturated soils 2006* (eds G. A. Miller, C. E. Zapata, S. L. Houston and D. G. Fredlund), GSP 147, pp. 2279–2290, https://doi.org/10.1061/40802(189)193. Reston, VA, USA: American Society of Civil Engineers.

Li, W. C., Dai, F. C., Wei, Y. Q., Wang, M. L., Min, H. & Lee, L. M. (2016). Implication of subsurface flow on rainfall-induced

landslide: a case study. *Landslides* **13**, No. 5, 1109–1123, https://doi.org/10.1007/s10346-015-0619-9.

Lim, T. T., Rahardjo, H., Chang, M. F. & Fredlund, D. G. (1996). Effect of rainfall on matric suctions in a residual soil slope. *Can. Geotech. J.* **33**, No. 4, 618–628, https://doi.org/10.1139/t96-087.

Lu, N. & Godt, J. (2008). Infinite slope stability under steady unsaturated seepage conditions. *Water Resour. Res.* **44**, No. 11, W11404, https://doi.org/10.1029/2008WR006976.

Lu, N. & Griffiths, D. V. (2004). Profiles of steady-state suction stress in unsaturated soils. *J. Geotech. Geoenviron. Engng* **130**, No. 10, 1063–1076, https://doi.org/10.1061/(ASCE)1090-0241(2004)130:10(1063).

Melchiorre, C. & Frattini, P. (2012). Modelling probability of rainfall-induced shallow landslides in a changing climate, Otta, Central Norway. *Clim. Change* **113**, No. 2, 413–436, https://doi.org/10.1007/s10584-011-0325-0.

Milledge, D. G., Griffiths, D. V., Lane, S. N. & Warburton, J. (2012). Limits on the validity of infinite length assumptions for modelling shallow landslides. *Earth Surf. Processes Landforms* **37**, No. 11, 1158–1166, https://doi.org/10.1002/esp.3235.

Sanzeni, A., Peli, M., Barontini, S. & Colleselli, F. (2019). Modelling of an accidentally triggered shallow landslide in Northern Italy. *Landslides* **16**, No. 11, 2277–2286, https://doi.org/10.1007/s10346-019-01251-2.

Sitarenios, P. & Casini, F. (2021). The hydromechanical interplay in the simplified three-dimensional limit equilibrium analyses of unsaturated slope stability. *Geosciences (Basel)* **11**, No. 2, article 73, https://doi.org/10.3390/geosciences11020073.

Skempton, A. W. & DeLory, F. A. (1957) Stability of natural slopes in London clay. In *Proceedings of the 4th international conference on soil mechanics and foundation engineering*, vol. 2, pp. 378–381. London, UK: Butterworths Scientific.

Travis, Q. B., Houston, S. L., Marinho, F. A. M. & Schmeeckle, M. (2010). Unsaturated infinite slope stability considering surface flux conditions. *J. Geotech. Geoenviron. Engng* **136**, No. 7, 963–974, https://doi.org/10.1061/(ASCE)GT.1943-5606.0000301.

Urciuoli, G., Pirone, M., Comegna, L. & Picarelli, L. (2016). Long-term investigations on the pore pressure regime in saturated and unsaturated sloping soils. *Engng Geol.* **212**, 98–119, https://doi.org/10.1016/j.enggeo.2016.07.018.

Ye, G., Zhang, F., Yashima, A., Sumi, T. & Ikemura, T. (2005). Numerical analyses on progressive failure of slope due to heavy rain with 2D and 3D fem. *Soils Found.* **45**, No. 2, 1–15, https://doi.org/10.3208/sandf.45.2_1.

Zhan, T. L. T., Jia, G. W., Chen, Y. M., Fredlund, D. G. & Li, H. (2013). An analytical solution for rainfall infiltration into an unsaturated infinite slope and its application to slope stability analysis. *Int. J. Numer. Analyt. Methods Geomech.* **37**, No. 12, 1737–1760, https://doi.org/10.1002/nag.2106.

Zieher, T., Schneider-Muntau, B. & Mergili, M. (2017). Are real-world shallow landslides reproducible by physically-based models? Four test cases in the Laternser valley, Vorarlberg (Austria). *Landslides* **14**, No. 6, 2009–2023, https://doi.org/10.1007/s10346-017-0840-9.